Freely available online OPEN ACCESS

BJR

RESEARCH

The combined use of kartogenin and platelet-rich plasma promotes fibrocartilage formation in the wounded rat Achilles tendon entheses

J. Zhang,
T. Yuan,
N. Zheng,
Y. Zhou,
M. V. Hogan,
J. H-C. Wang

University of Pittsburgh, Pittsburgh, Pennsylvania, United States

Objectives

After an injury, the biological reattachment of tendon to bone is a challenge because healing takes place between a soft (tendon) and a hard (bone) tissue. Even after healing, the transition zone in the enthesis is not completely regenerated, making it susceptible to re-injury. In this study, we aimed to regenerate Achilles tendon entheses (ATEs) in wounded rats using a combination of kartogenin (KGN) and platelet-rich plasma (PRP).

Methods

Wounds created in rat ATEs were given three different treatments: kartogenin platelet-rich plasma (KGN-PRP); PRP; or saline (control), followed by histological and immunochemical analyses, and mechanical testing of the rat ATEs after three months of healing.

Results

Histological analysis showed well organised arrangement of collagen fibres and proteoglycan formation in the wounded ATEs in the KGN-PRP group. Furthermore, immunohistochemical analysis revealed fibrocartilage formation in the KGN-PRP-treated ATEs, evidenced by the presence of both collagen I and II in the healed ATE. Larger positively stained collagen III areas were found in both PRP and saline groups than those in the KGN-PRP group. Chondrocyte-related genes, SOX9 and collagen II, and tenocyte-related genes, collagen I and scleraxis (SCX), were also upregulated by KGN-PRP. Moreover, mechanical testing results showed higher ultimate tensile strength in the KGN-PRP group than in the saline control group. In contrast, PRP treatment appeared to have healed the injured ATE but induced no apparent formation of fibrocartilage. The saline-treated group showed poor healing without fibrocartilage tissue formation in the ATEs.

Conclusions

Our results show that injection of KGN-PRP induces fibrocartilage formation in the wounded rat ATEs. Hence, KGN-PRP may be a clinically relevant, biological approach to regenerate injured enthesis effectively.

Cite this article: *Bone Joint Res* 2017;6:231–244

Keywords: Enthesis, fibrocartilage, tendon-bone junction, kartogenin, platelet-rich plasma

Article focus

- Our primary aim in this study was to regenerate the wounded rat Achilles tendon entheses (ATEs) by combining the use of KGN with PRP.
- We also investigated whether treatment of wounded ATEs with PRP alone can result in the formation of fibrocartilage in the injured region.

Key messages

- KGN, together with PRP, can regenerate the enthesis in wounded ATE by promoting fibrocartilage formation in the injured region.
- KGN can be used as a mode of cell-free therapy to promote fibrocartilage formation in damaged entheses in clinical settings.

J. Zhang, PhD, Research Associate Professor,
T. Yuan, MD, PhD, Research Fellow,
Y. Zhou, MD, Research Fellow,
M. V. Hogan, MD, Assistant Professor,
J. H-C. Wang, PhD, Professor, Department of Orthopaedic Surgery, University of Pittsburgh School of Medicine, 200 Lothrop Street, Pittsburgh, Pennsylvania 15213, USA.
N. Zheng, PhD, Associate Professor, Department of Mechanical Engineering, University of North Carolina, 9201 University City Blvd, Mechanical Engineering, Duke 201, Charlotte, North Carolina, USA.

Correspondence should be sent to J. H-C. Wang;
email: wanghc@pitt.edu

doi: 10.1302/2046-3758.64.BJR-2017-0268.R1

Bone Joint Res 2017;6:231–244.
Received: 07 October 2016;
Accepted: 10 February 2017

- Treatment with PRP alone cannot restore normal structure to wounded enthesis because it does not induce fibrocartilage formation.

Strengths and limitations

- This is a partial injury model, where a small 1 mm diameter injury was created in a localized manner using a biopsy punch.
- We assessed only one KGN and PRP concentration.
- Future studies will address optimization of KGN and PRP levels required for effective fibrocartilage formation.

Introduction

In mammalian joints, tendons and ligaments are attached to bones through a transition zone called the enthesis.[1-3] The enthesis is made of a fibrocartilage transition zone, which is uncalcified on the portion proximal to the tendon, but is calcified on the side proximal to the bone. The main function of the fibrocartilage transition zone is to absorb stress during mechanical loading and thus protect tendons from injury.[1] In the event of an injury, however, the transition zone in the enthesis is not effectively restored to its native form because of a lack of fibrocartilage regeneration.[2,3] Previous attempts to regenerate enthesis in animal models post-surgery have resulted in the formation of scar tissue in tendon-bone junctions[4-7] that has inferior mechanical properties. As a result, the ability to withstand mechanical loads is reduced, thereby leading to re-injuries.[2,8] Therefore, regenerating the enthesis is a common clinical problem, and current approaches for engineering tissue using cells (mesenchymal stem cells (MSCs))[9,10] and scaffolds (hybrid silk,[9] nanofibre,[11]) have achieved only limited success in this area.[12]

Recently, two tissue engineering approaches have gained popularity in the treatment of tendon injuries. The first is platelet-rich plasma (PRP) which has been widely used in the clinical treatment of injured tendons[13] and other musculoskeletal tissue injuries.[14] PRP contains multiple growth factors and, when injected into the injured region, PRP promotes wound healing by increasing cell proliferation and collagen production,[15-17] and decreasing inflammation.[18] These growth factors include platelet-derived growth factor (PDGF), transforming growth factor-β (TGF-β), vascular endothelial growth factor (VEGF), epidermal growth factor (EGF), insulin-like growth factor-1 (IGF-1), fibroblastic growth factor (FGF), and hepatocyte growth factor (HGF).[19,20] Currently, most pre-clinical PRP studies have focused on tendon mid-substance injuries instead of tendon-bone junction injuries. While PRP is known to induce cartilage formation in animal models with cartilage defects,[21,22] whether PRP can also promote fibrocartilage formation and hence enable regeneration of the wounded enthesis in the tendon-bone interface has not been clearly demonstrated.

The second, a small compound called kartogenin (KGN), was shown to promote robust chondrocyte differentiation of primary mouse mesenchymal stem cells (MSCs).[23] In a previous study, we showed that a short-term (two weeks) KGN treatment of tendon stem/progenitor cells (TSCs) *in vitro* and injection of KGN into tendon wounds *in vivo* promoted chondrogenesis of TSCs and induced cartilage-like tissue formation in rat tendons, respectively.[24] The results from this KGN injection approach indicated that, without a carrier, cartilage-like tissue would be formed in the soft tissue such as tendons due to the leakage of KGN solution. Our recent study further revealed the ability of KGN, along with PRP, to induce fibrocartilage zone formation in a rat tendon graft-bone tunnel model.[25] Although PRP is known to augment tissue healing when combined with tissue engineering modalities such as TSCs and bone mesenchymal cells (BMCs),[26-28] it is not known whether PRP and KGN, either alone or in combination, can effectively regenerate an injured enthesis.

In this study, we aimed to regenerate enthesis in a wounded rat Achilles tendon enthesis (ATE) by combining the use of KGN with PRP (KGN-PRP). Specifically, we injected KGN-PRP into the wounded rat ATE, and determined its long-term effects three months after the treatment. It is known that PRP can enhance healing of injured tissues.[13] For PRP to have such a "healing effect," the bioactive factors that are stored in platelets must be released by activation.[19,20] This is typically done by mixing the PRP preparation with thrombin or $CaCl_2$ *in vitro*, or when PRP comes into contact with collagen *in vivo*.[14,29-31] In both cases, activated PRP forms a gel, which serves as a carrier of KGN, and allows not only the delivery of KGN into the wound area but also prevents the diffusion of KGN that may cause unintended cartilage-like tissue formation in neighbouring tissues.[24]

Materials and methods

All experimental protocols for the use of rats in this study were approved by the University of Pittsburgh. Efforts were made to minimise pain and suffering to animals during experimentation.

Preparation of Autologous PRP. PRP was prepared as described previously in our published protocol in a two-step centrifugation process.[32] Briefly, whole blood (0.9 ml) was extracted from the heart of each Sprague Dawley rat (three months old and weighing 230 g to 270 g) using a 21-gauge needle and mixed with 0.1 M sodium citrate (0.1 ml) in a centrifuge tube. Blood was centrifuged at 500 g for ten minutes, which yielded three layers (Fig. 1a). The top layer was centrifuged again at 2200 g for an additional ten minutes. The supernatant was collected as platelet-poor plasma (PPP) and the pellet was retrieved along with a small quantity of PPP and referred to as PRP (Fig. 1a). Platelets in PRP were counted

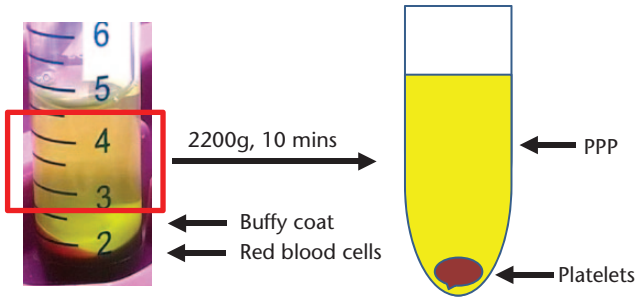

Fig.1a

Fig.1b

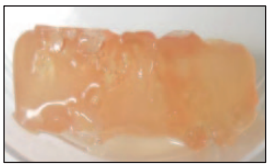

Fig.1c

Preparation of kartogenin platelet-rich plasma (KGN-PRP) gel and PRP gel. a) Whole blood from each rat used in three experimental groups was separated into three layers after centrifugation at 500 g for ten minutes. A second centrifugation of the supernatant (red box) at 2200 g for ten minutes yielded platelet-poor plasma (PPP) and the platelet pellet. PRP was prepared by re-suspending the platelets in a small volume of PPP and diluted further with PPP, such that the platelet concentration was about three times higher than that found in whole blood. b) A typical KGN-PRP gel made by adding thrombin to a mixture of PRP and KGN. c) A typical PRP gel obtained by adding thrombin to PRP.

using the CELL-DYN Emerald System (Abbott Diagnostics, Lake Forest, Illinois). Platelet concentration in PRP was adjusted to 5.67 ± 1.17×10^8/ml, three times higher than the baseline level in whole blood (1.89 ± 0.55×10^8/ml) using PPP and used in the following experiments. Our previous study showed that a platelet concentration in PRP preparations with about three-fold over baseline value of whole blood is sufficient in stimulating TSC proliferation and differentiation.[32]

Preparation of KGN-PRP gel and PRP gel. KGN (5 mg; Sigma-Aldrich, St. Louis, Missouri) was dissolved in 0.3 ml dimethyl sulfoxide (DMSO) to make a 50 mM KGN stock solution, which was diluted with double distilled water to obtain 1 mM or 5 mM KGN working solutions. KGN-PRP gel was then prepared by mixing 10 µl of the 5 mM KGN solution, 0.5 ml of PRP from above and 10 µl of 10 000 U/ml bovine thrombin, which was used to activate platelets. Therefore, each piece of KGN-PRP gel contained 10 µl of 5 mM KGN equivalent to 100 µM of KGN-PRP gel. PRP gel was prepared in the same manner as KGN-PRP gel except that it contained no KGN.

Determination of KGN release from KGN-PRP gel. One KGN-PRP gel prepared as above was incubated at 37°C in 10 ml phosphate-buffered saline (PBS) with continuous rotation in a micro-hybridisation incubator (Robbins Scientific, Sunnyvale, California) for seven days. About ten such gels were incubated individually in PBS. Then, at different time points (one, two, four, eight hours, and up to seven days), 100 µl of PBS was retrieved and an equal amount of fresh PBS was replaced. KGN in PBS was then quantified using high performance liquid chromatography (HPLC) (Agilent 1100 HPLC System; Agilent Technologies, Santa Clara, California), consisting of a quaternary pump, auto-injector, online degasser and UV detector. Each 20 µl sample was passed through a 0.5 µm pre-column filter (Waters Corp., Milford, Massachusetts) and injected into an Athena C_{18} column (250 × 4.6 mm inner diameter (i.d.), 5 µm). The mobile phase consisted of acetonitrile (buffer A) and water (buffer B), both containing 0.1% H_3PO_4. Gradient elution was carried out at a flow rate of 0.4 ml/min, and the mobile phase gradient was ramped linearly from 10% buffer A to 95% buffer A over ten minutes. Samples were held in this buffer (95% buffer A and 5% buffer B) for ten minutes and returned to 10% buffer A for one minute followed by a last ten-minute hold. The system was allowed to equilibrate for eight minutes before the next injection. The amount of KGN in PBS was detected at 280 nm and was deemed to be the amount released from the KGN-PRP gel. The concentration of KGN released from KGN-PRP gel was calculated using a standard curve made from various concentrations of pure KGN solutions (R^2 = 0.996). The KGN release efficiency was calculated as a percentage as follows: Percentage (%) of KGN = $KGN_{(in\ PBS)}$ / $KGN_{(initial\ KGN\ in\ the\ KGN\text{-}PRP\ gel)}$ × 100%.[33]

In vivo animal experiment. Before starting the *in vivo* experiments, the sample size (eight rats/each group) for mechanical testing was estimated using a power of 85%, a type one error 0.05 and a 100% treatment effect size in terms of tendon stiffness. The sample size (6 rats/group) for histologic and immunohistochemical analyses was estimated based on the need for repeated analyses as well as our experience. A total of 42 Sprague Dawley rats (female, three months old) were used in the *in vivo* experiments. First, all rats were anaesthetised and the skin was opened to expose the Achilles tendon-bone region. Then, a biopsy punch (Miltex Inc., York, Pennsylvania) angled transversely at the ATE was used to create a wound in the ATEs of both hind legs. The width of a rat ATE in this study was about 3 mm and the biopsy punch made a 1 mm diameter wound at the centre of the ATE (Figs. 2a and 2b). In the injury model, the mineralised zone of ATE and bone beneath avoided damaged by controlling the depth of 'pushing' the punch downward. The wounded rats were then randomly divided into three groups with 14 rats in each group. All of the rats in each group received the following treatments directly into the wounds created in both legs. Group 1, the KGN-PRP group, was injected with a solution containing 3 µl of KGN (1 mM), 22 µl of PRP and 5 µl of 10 × 10^3 U/ml thrombin (KGN-PRP); Group 2, the PRP-treated group, was injected with 3 µl of DMSO, 22 µl of PRP and 5 µl of 10 × 10^3 U/ml thrombin (PRP); and Group 3, the control, received 3 µl of DMSO and 27 µl of saline injected into

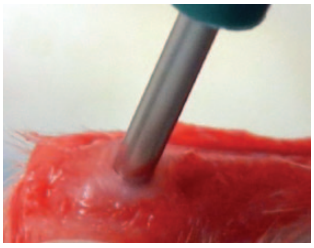

Fig. 2a

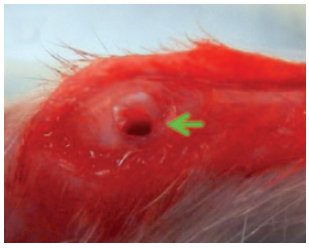

Fig. 2b

Fig. 2c

Fig. 2d

Fig. 2e

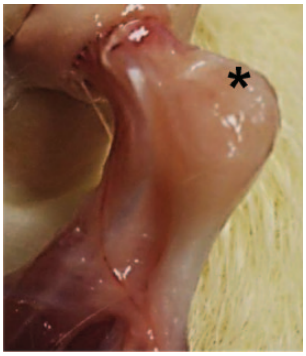

Fig. 2f

Images showing the gross examination of the effect of kartogenin platelet-rich plasma (KGN-PRP) on the healing of wounded rat Achilles tendon entheses (ATEs). a) A 1 mm diameter wound was made in the rat ATE (3 mm total width) using a biopsy punch. b) Wound in the rat ATE. c) Wounded rat ATE 3 months after KGN-PRP treatment. d) An intact rat ATE. e) Wounded rat ATE after PRP treatment shows a wound healing site with uneven surface (arrow). f) Wounded rat ATE after saline treatment also shows incomplete healing with a rough surface and smaller healed region and reddish immature tissues (*).

each wounded leg (Saline). The final concentration of KGN injected into the wounded ATE was 100 μM. In the PRP- and saline-treated groups, trace amounts of DMSO (3 μl/each wound) were also added so that the amount of DMSO solvent remained the same in all three groups. The skin was then sutured and on day 90 post-surgery (three months), all rats were killed by inhalation of CO_2, and their ATEs from both legs were collected for gross inspection followed by histochemical analysis (right legs from six rats/group, n = 18), gene expression analysis (left legs from six rats/group, n = 18) and mechanical testing (both legs from eight rats/group, n = 48). During the experimental period, all rats were allowed free roam in cages, and no complications or infections were noted in any of rats. Also note that three un-wounded rats were used for demonstrating their intact ATEs (Fig. 2).

Histochemical analyses. For histochemical analysis, rat ATEs (right legs from six rats/group, n = 6), were harvested three months post-surgery and immersed in frozen section medium (Neg 50; Richard-Allan Scientific, Kalamazoo, Michigan) in pre-labeled base moulds. The samples were then flash-frozen by placing them in 2-methylbutane chilled in liquid nitrogen. The frozen tissue blocks were stored at -80°C until required. Each frozen tissue section was cut into sections 8 μm thick and placed on glass slides to dry overnight at room temperature, and then fixed in 4% paraformaldehyde for 15 minutes and stained with haematoxylin and eosin (H&E). Additional tissue sections were also stained with Safranin O, to identify proteoglycan and glycosaminoglycans and Fast Green to identify collagen (S&F) according to our published protocol.[18] All stained sections were observed through a microscope (Nikon Eclipse TE2000-U; Nikon Instruments Inc., Melville, New York). Each slide was viewed and scored by three laboratory persons (JZ, TY, and YZ) who were blinded to treatment allocation, i.e., they did not know whether the slide samples were from a treated or untreated group. The semi-quantification was done to evaluate the extent of fibrocartilage formation in each group. The percentage of fibrocartilage-like tissue in whole tissue was used as a scoring scale according to the published method but with a slight modification:[34] Score 0, the percentage of positive stained tissue is less than 9%; score 1, the percentage of positive stained tissue is more than 10% but less than 24%; score 2, the positive stained tissue is more than 25% but less than 34%; score 3, the positive stained tissue is more than 35% but less than 49%; score 4, the positive stained tissue is more than 50% but less than 64%; score 5, the positive stained tissue is more than 65%. A total of 18 ATE sections were analysed for each marker (e.g. collagen II) in each group.

Immunofluorescence staining. The frozen rat ATEs cut into sections 8 μm thick were first fixed in 4% paraformaldehyde for 15 minutes at room temperature. After washing in PBS, ATE sections from treated and untreated groups were incubated overnight in five different primary antibodies at 4°C; one group was incubated with mouse anti-collagen I (1:300; Millipore, Billerica, Massachusetts) and rabbit anti-collagen II together (1:300; Abcam, Cambridge, Massachusetts); the other group was incubated with rabbit anti-SOX9 (1:500; Millipore, Billerica, Massachusetts) and goat anti-scleraxis together (SCX) (1:300; Santa Cruz Biotechnology, Inc., Dallas, Texas). Additionally, ATE sections were stained with rabbit anti-collagen III antibody (1:200; Abcam, Cambridge, Massachusetts). The slides were then rinsed three times in PBS and incubated with the following secondary antibodies at room temperature for two hours: FITC-conjugated goat anti-mouse IgG (1:500; Abcam,

Cambridge, Massachusetts) to detect collagen I, Cy3-conjugated goat anti-rabbit IgG (1:500; Abcam) to detect collagen II, FITC-conjugated donkey anti-goat IgG (1:500; Abcam, Cambridge, Massachusetts) to detect SCX and Cy3-conjugated donkey anti-rabbit IgG (1:500; Abcam, Cambridge, Massachusetts) to detect SOX9 and collagen III. Excess secondary antibody was removed by washing in PBS. Finally, stained tissue sections were observed through a fluorescence microscope (Eclipse TE2000-U).

Quantitative real-time polymerase chain reaction (RT-PCR). qRT-PCR was performed according to standard protocols. Briefly, total RNA was extracted separately from each rat ATE (left legs from six rats/group, n = 18) using the RNeasy Mini Kit (Qiagen Inc., Valencia, California), and first strand cDNA was synthesised using SuperScript II Reverse Transcriptase' (Invitrogen, Grand Island, New York) according to the manufacturer's instructions. Then, about 2 µl of the first strand cDNA (total 100 ng RNA) was used to perform qRT-PCR using the QuantiTect SYBR Green PCR Kit (Qiagen) and carried out in a Chromo 4 Detector (MJ Research, St. Bruno, Quebec, Canada). Samples were incubated for five minutes at 94°C, followed by 40 cycles at 94°C for one minute, 57°C for 40 seconds and 72°C for 50 seconds, and a final incubation at 70°C for ten minutes. Rat-specific primers were used to perform gene expression in the ATE: three chondrocyte-related genes: aggrecan, collagen II and SOX9; a tenocyte-related gene: tenomodulin; and fat- and bone-related genes: PPARγ, osteocalcin and RUNX2.[35] Glyceraldehyde 3-phosphate dehydrogenase (GAPDH) was used as the reference gene. All primers were synthesized by Invitrogen (Waltham, Massachusetts). Relative gene expression levels were estimated using the $2^{-\Delta\Delta CT}$ method, where $\Delta\Delta CT = (CT_{target} - CT_{GAPDH})_{treatment} - (CT_{target} - CT_{GAPDH})_{control}$ and CT represents the threshold cycle of each RNA sample. Each gene from each group was amplified three times and all three CT values were used to determine the mean gene expression level.

Mechanical testing. Whole right and left legs from eight rats in each of the 3 groups (n = 48) were used for mechanical testing. The dissected specimens were wrapped in tissue paper moistened with PBS and stored individually in sealed plastic bags at -20°C. Prior to mechanical testing, the legs were thawed to room temperature according to the published protocol.[36] The rat leg was secured such that the foot was fixed on a metal platform, whereas the Achilles tendon on the proximal end of the specimen was fixed to the testing machine (ElectroForce 3200; TA Instruments, Eden Prairie, Minnesota) with a tendon clamp. The tendon was aligned parallel to the movement direction of the actuator in the testing machine. A load cell with a measurement range up to 225 N was used to measure tensile loads. The mechanical testing was done at a loading rate of 10 mm per minute until failure at room temperature.[10] Note that in this study we used the breaking strength at the tendon insertion site to estimate the ability of the healed ATE to withstand tensile mechanical load.

Statistical analysis. The data from qRT-PCR and mechanical testing were analysed using one-way ANOVA, followed by Fisher's least-significant difference (LSD) test for multiple comparisons. When p-values were less than 0.05, the two groups being compared were considered to be significantly different.

Results

To determine the effect of the KGN-PRP combination on the healing of wounded rat entheses, we delivered a PRP gel with and without KGN into the wounded rat ATEs. Typically, un-activated PRP is in a liquid form but after activation by adding thrombin, a soft gel is formed within five minutes. Also, the KGN-PRP gel, which contained KGN, did not exhibit apparent differences from the PRP gel (Figs 1b and 1c). Note that these gels are mainly made of fibrin, which is very compliant and easily degraded by enzymes *in vivo*.[37]

Prior to injecting the KGN-PRP gel for *in vivo* evaluation, we first determined through HPLC whether KGN is released from the KGN-PRP gel by incubating the gel in PBS *in vitro*. A typical HPLC chromatograph of a KGN standard showed that the retention time of KGN was 21 minutes (Fig. 3a). A similar peak at 21 minutes was also recovered from the PBS solution where a KGN-PRP gel was left incubating for 24 hours (Figs. 3b and 4b), indicating the release of KGN from the gel. Furthermore, the *in vitro* kinetics experiments indicated that almost 95% of the KGN was released from the PRP gel during the first eight hours of incubation in PBS at 37°C (Fig. 4a). Almost 100% of the KGN was released into the PBS *in vitro* within two days of incubation, and the KGN concentration in PBS remained constant for the following seven days (Fig. 4b). These results suggest that PRP is an excellent carrier for the rapid delivery of KGN into a target tissue without KGN degradation for at least several days.

Next, we examined the effect of KGN-PRP on the healing of wounded rat ATEs by injecting KGN-PRP gel, PRP gel or saline into the wounds (Figs. 2a and 2b). Three months after treatment, morphological observations of the rat hind legs showed normal appearance with a smooth surface only in the KGN-PRP-treated rat ATEs (Fig. 2c), which were similar to intact ATEs without wounding (Fig. 2d). In contrast, both PRP- (Fig. 2e) and saline- (Fig. 2f) treated ATEs appeared to have healed although the healed tissue had an uneven surface, with crests and troughs. Such a rough appearance was observed in all PRP- and saline-treated ATEs. The saline-treated ATE also appeared reddish, suggesting the presence of immature tissue.

Histochemical analysis by H&E staining showed a well organised parallel arrangement of collagen fibres and

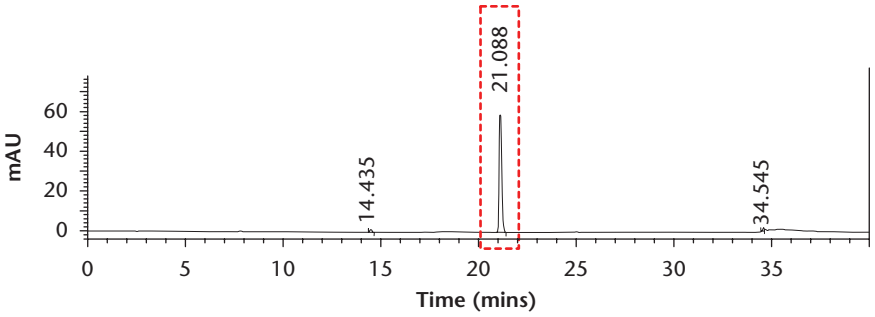

Fig.3a

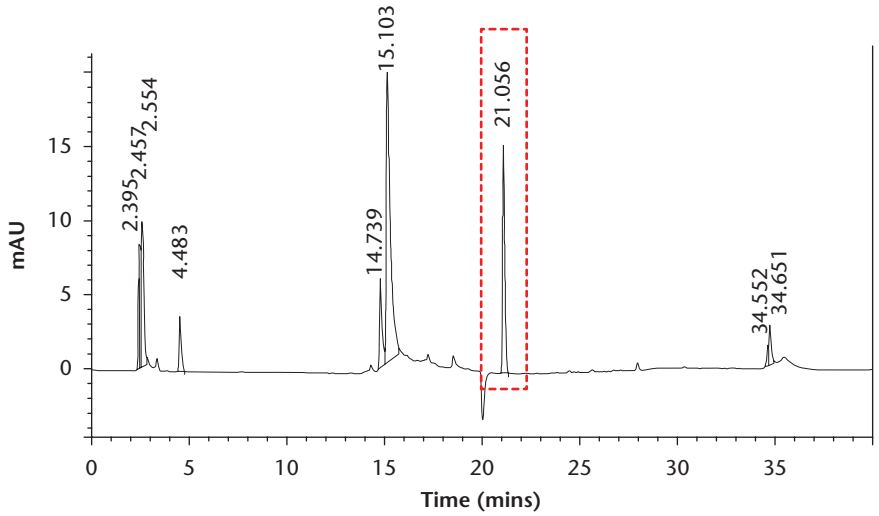

Fig.3b

Using HPLC chromatographs to determine KGN release from PRP gel. A typical chromatograph of a 10 µg/ml KGN standard (a); Chromatogram of the PBS solution after incubating a KGN-PRP gel for 24 hrs (b). The peak eluted at 21 min (red box) and corresponding to the single highest peak in A (red box) represents the KGN released into the PBS from the KGN-PRP gel.

apparent chondrocytes in the KGN-PRP-treated group (Fig. 5a). The KGN-PRP-treated group contained chondrocytes similar to those found in uninjured ATEs (Fig. 5b). In ATEs treated with PRP alone, a transition zone was evident with a moderate arrangement of fibres, and the ATEs appeared completely healed (Fig. 5c) but no chondrocytes were apparent. In contrast, the saline-treated ATEs exhibited poor organisation of fibres and cells, which were not chondrocyte-like (Fig. 5d). Moreover, a few gaps, which were consistently present in all the ATE sections of this group, were also observed, indicating that in this group wound healing was incomplete (Fig. 5d). Further histochemical staining with Safranin O and Fast Green showed the presence of proteoglycans (red), as well as mature chondrocytes, only in the KGN-PRP-treated ATE (Fig. 6), indicating that a cartilage-like transition zone had formed due to KGN-PRP treatment (Fig. 6a), which was similar to that of the intact rat ATE (Fig. 6b). PRP, on the other hand, induced some proteoglycan expression in the ATEs (Fig. 6c). In contrast, the saline-treated group (Fig. 6d) did not have any proteoglycan, indicating the lack of cartilage-like tissue formation in this group in addition to the irregular arrangement of cells.

In addition, positive staining for collagen I and collagen II was identified by immunostaining only in the KGN-PRP-treated ATE, thus verifying that the newly formed cartilage-like tissue was indeed fibrocartilage (Figs. 7a and 7b). Superimposed collagen I (green) and collagen II (red) positive images clearly showed the presence of both types of staining in the same region (Figs 7c and 7d), thus further confirming that these orange/yellow regions are the newly formed fibrocartilage. Moreover, both the KGN-PRP group (Figs 7a to 7d) and the intact group (Figs 7m to 7p) exhibited positive staining of collagen I and II. In contrast, the PRP-treated ATE had some collagen I expression (Fig. 7e) but collagen II was almost non-existent (Fig. 7f) and no region in the tendon-bone transition zone contained both collagen I and collagen II (Figs. 7g and 7h). In the saline-treated group, although collagen I was present in abundance, collagen II was absent in the healed ATE (Figs. 7i to 7l).

Immunostaining with SCX and SOX9 antibodies corroborated these findings; that is, the KGN-PRP treatment

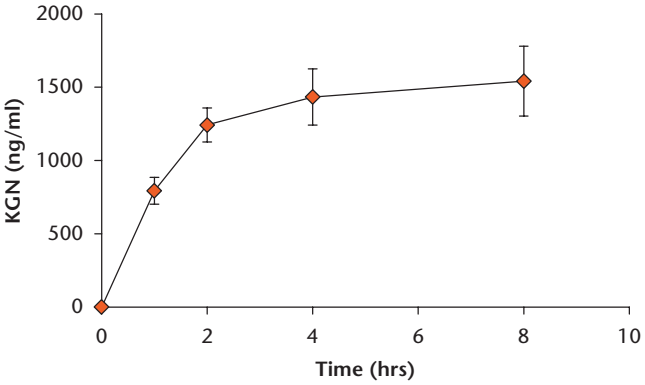

Fig. 4a

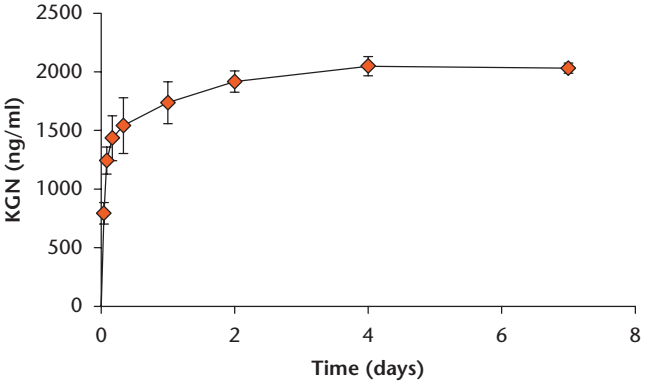

Fig. 4b

Kartogenin (KGN) release kinetics from KGN- PRP gel *in vitro*. a) The time course of KGN release, measured by HPLC chromatographs, in the initial eight hours *in vitro*. b) Release of KGN from KGN-PRP gel during seven days *in vitro*. KGN-PRP gels were individually placed in PBS at 37°C and an aliquot of the solution was removed at the indicated time points to measure the amount of KGN released into the phosphate-buffered solution (PBS). It is evident that > 90% of KGN was released within the first eight hours.

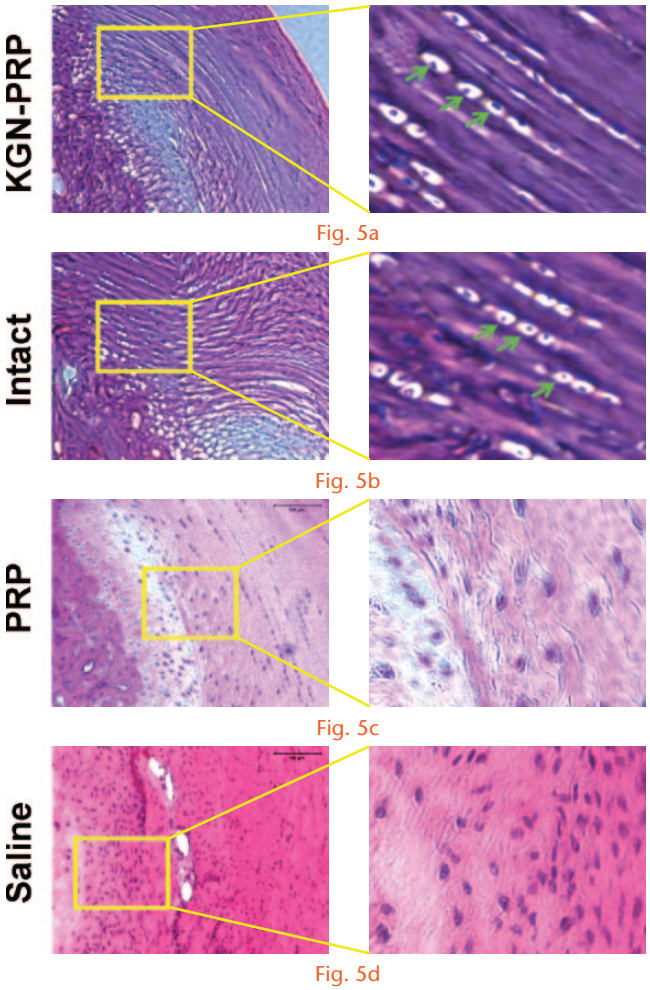

Fig. 5a

Fig. 5b

Fig. 5c

Fig. 5d

Kartogenin-platelet-rich plasma (KGN-PRP) treatment results in well organised collagen fibres in the healing site of wounded rat Achilles tendon enthe-ses (ATE). KGN-PRP-treated ATE (a) shows well organised arrangement of collagen fibres; moreover, mature chondrocytes that align with collagen fibres are present in the transition zone between tendon and bone (arrows), which are similar to those of intact rat ATEs (b). The PRP-treated ATE (c) has less organised collagen fibres; and saline-treated ATE (d) reveals defects in the healed ATE evidenced by gaps. In both PRP and saline groups, formation of chondrocytes is not apparent, and cell organization is also random.

resulted in the expression of SCX, a tendon cell marker (Fig. 8a) as well as SOX9, a chondrocyte marker (Fig. 8b). Superimposing the two SCX and SOX9 positive images clearly showed the same cells expressing both SCX and SOX9 (yellow, Figs 8c and 8d), indicating that these are "fibrocartilage cells" in the fibrocartilage region, which were similar to those cells in intact rat ATEs (Figs. 8m to 8p). After PRP treatment, robust expression of SCX was observed (Fig. 8e), but SOX9 expression was only moder-ate (Fig. 8f). Merging the two images clearly showed the presence of fewer orange/yellow cells compared with the KGN-PRP group. Since collagen II was nearly absent in the PRP-treated group (Fig. 7f), these orange/yellow cells may be immature “fibrocartilage cells” (Figs. 8g to 8h). These results reveal that PRP alone cannot effectively induce the formation of fibrocartilage in the healed ATE. Moreover, the saline-treated ATE stained positive for SCX (Fig. 8I), but negative for SOX9 (Fig. 8J) proteins, indicating the lack of fibrocartilage formation in the saline-treated group (Figs. 8k and 8l). Finally, much stronger expression of collagen III was found in both the PRP-treated group (Figs. 9e to 9h) and the saline-treated group (Figs 9i to 9l) than was found in the KGN-PRP-treated group (Figs 9a to 9d) and intact (uninjured) ATEs (Figs. 9m to 9p). All stained sections were analysed using the scoring scale described above, and the consensus scores from 3 reviewers are shown in Table I.

Quantitative RT-PCR was performed to analyse the expression of three categories of genes. First, the chondrocyte-related genes, SOX9, collagen II and aggre-can were significantly upregulated ($p < 0.05$) only in the KGN-PRP group but not in the PRP- or saline-treated groups (Fig. 10a). SOX9 increased 3.4-fold, collagen II 5.7-fold and aggrecan 6.6-fold when compared with the saline-treated group. All three gene expression levels were similar between the saline-and PRP-treated groups. Second, expression of the tenocyte-related gene, tenom-odulin, was upregulated 1.9- and 1.3-fold in the KGN-PRP- and PRP-treated groups ($p < 0.05$), respectively

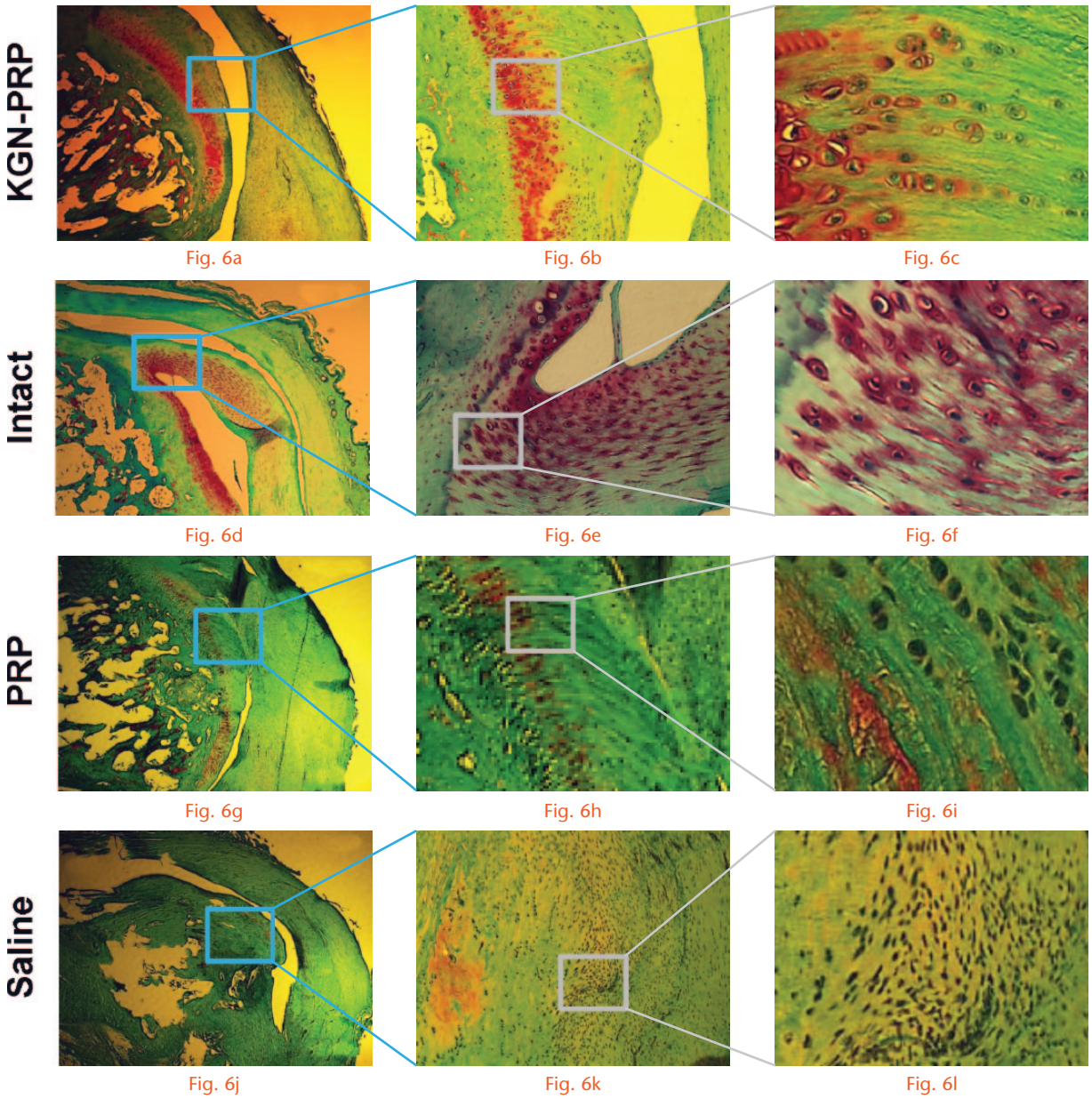

Kartogenin platelet rich plasma (KGN-PRP) treatment results in the formation of proteoglycans in a wounded rat Achilles tendon enthesis (ATE). (a to c) KGN-PRP treated ATE wound; (d to f) Intact rat ATE; (g to i) PRP treated ATE wound; (j to l) Saline treated wound. The images of b, e, h and k are enlarged views of blue boxes in a, d, g and j, whereas the images of c, f, i and l are enlarged views of white boxes in b, e, h and k. KGN-PRP treatment induces extensive production of proteoglycan (b, red dots) and exhibits a similar pattern of that of intact rat ATEs, unlike PRP and saline treatments, which induce little proteoglycan production. Note that the large gaps in a, b, d, e, g and j are due to the separation of soft tissue (tendon) from hard tissue (newly formed enthesis) during sectioning. Safranin O and Fast Green staining. Scale Bars: 500 μm (blue bars in a, d, g, and j); 200 μm (white bars in b, e, h, and k); 25 μm (red bars in c, f, i and l).

(Fig. 10b). Third, the expression of non-tenocyte-related genes, PPARγ (adipocyte marker), osteocalcin and RUNX2 (bone markers), was low and did not significantly differ among the three groups (Fig. 10c). Together, these results indicate that only KGN-PRP treatment in the three groups still induced fibrocartilage-related gene expression in wounded rat ATEs after three months of healing.

Finally, in the KGN-PRP-treated group, the maximum failure load increased by 31.5% in comparison with the saline-treated samples, whereas the maximum failure load of the PRP-treated group was 44.4% higher than the saline-treated group (Fig. 11). Note that during mechanical testing, technical problems such as tendon slips were noticed in some of the 16 ATE specimens in each group and these were not included in the analysis because their values did not represent the mechanical strengths of healed entheses due to KGN-PRP, PRP or saline treatment. The final numbers of the specimens in each group are as follows: KGN-PRP: 14; PRP: 12; and saline control: 8.

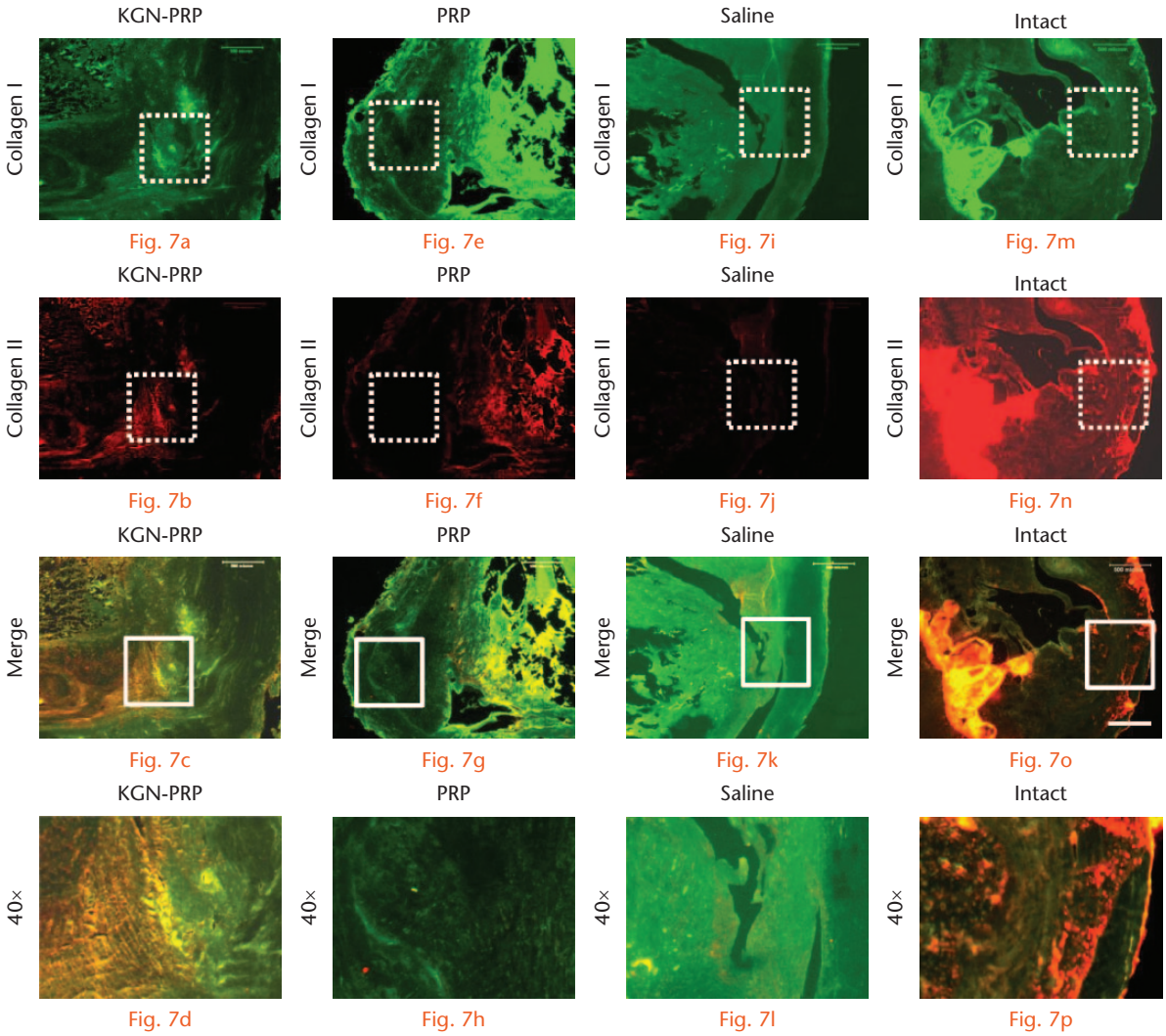

Immunochemical staining showing the effect of kartogenin-platelet-rich plasma (KGN-PRP) treatment on the expression of both collagen I and collagen II in the healed Achilles tendon entheses (ATEs). KGN-PRP treatment induces the expression of both a) collagen I, and b) collagen II. Merging the two images shows orange/yellow staining (c), indicating the presence of both collagen I and collagen II at the same region (dashed squares), which is typical for fibrocartilage tissues also shown in intact rat ATEs (m, n, o, p). In contrast, collagen I is present in moderation in the PRP- (e, f, g, h) and saline- (i, j, k, l) treated ATEs, but collagen II is almost non-existent in both groups. These results indicate that both PRP and saline treatments result in the absence of fibrocartilage in the healed ATEs. The images of d, h, l and p are enlarged views of the white boxes in c, g, k and o, respectively.

Discussion

In this study, we used a combination of KGN with PRP to regenerate wounded rat ATEs. Delivery of KGN-PRP gel into wounded rat ATEs effectively healed the injury and promoted better "quality healing" of wounded rat ATEs than in the groups treated either with PRP or saline. The KGN-PRP-treated rat ATE appeared similar to the intact ATE. It also resulted in well organised collagen fibres, robust production of proteoglycans and increased expression of both collagen I and collagen II proteins. Fibrocartilage cells expressing both SCX and SOX9 proteins were also identified in the KGN-PRP-treated group, but not in the PRP- or saline-treated groups. Finally, the mechanical strength of the healed ATE was significantly higher than that of the saline-treated group. Taken together, these results indicate that KGN, when combined with PRP, not only enhances healing, but also promotes the regeneration of the fibrocartilage zone in the wounded rat ATE.

From this study, it is clear that PRP treatment alone did poorly in promoting the formation of fibrocartilage in wounded rat ATEs. However, it did enhance healing by inducing collagen I expression (Fig. 7). The results indicate that collagen I fibres were formed in the wounded rat ATEs due to PRP treatment. This may partially explain why PRP treatment increased the tensile mechanical strength (maximum failure load) of the wounded ATE compared with saline treatment, which had a negative effect on the healing of wounded ATE. However, the tissues in the healed ATEs of the PRP group are of inferior quality because, like the saline group, it contained scar tissue formation, characterised by the presence of

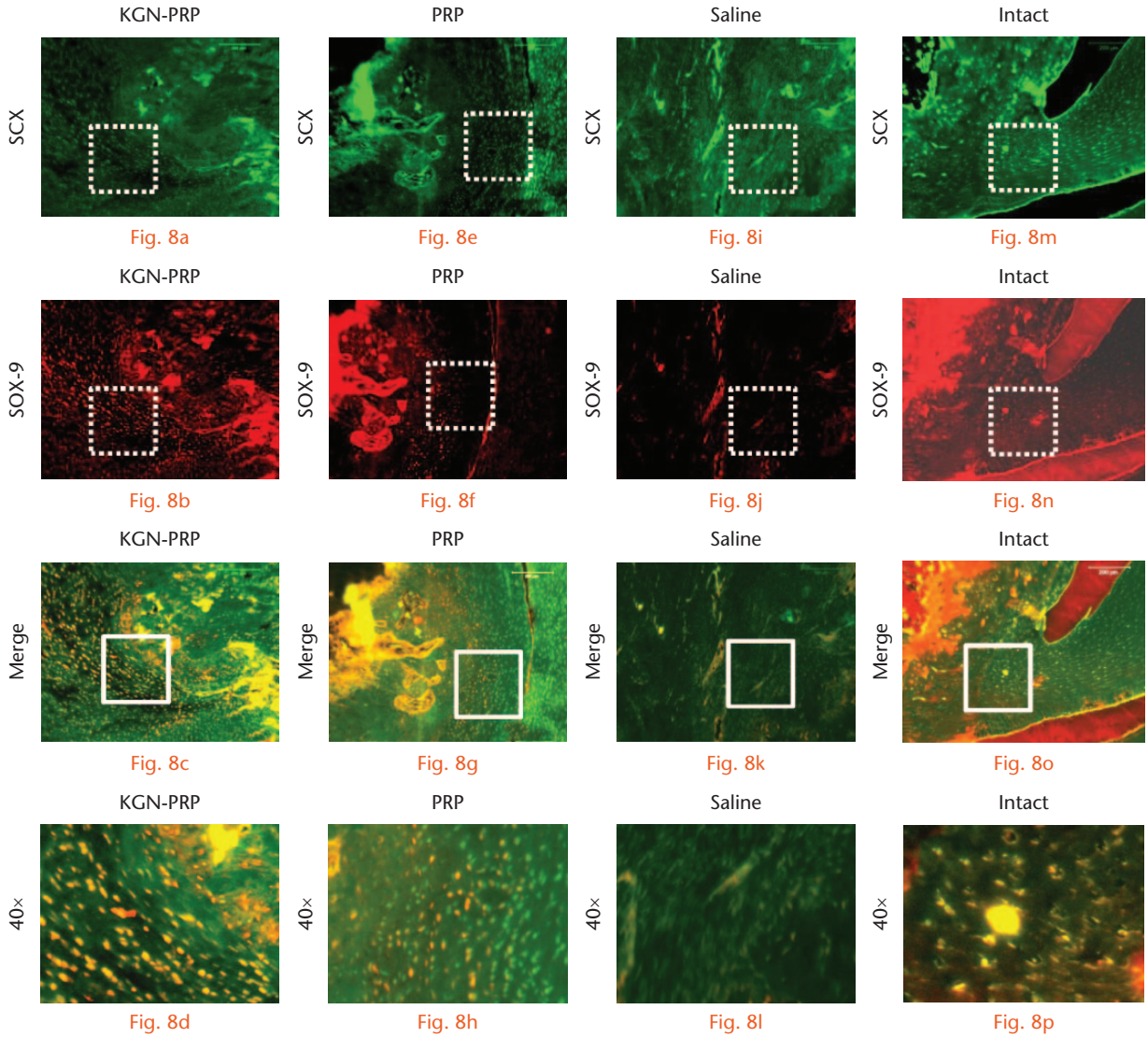

The effect of Kartogenin-platelet-rich plasma (KGN-PRP) treatment on SCX and SOX9 expression in the healed Achilles tendon entheses (ATEs). KGN-PRP treatment increases the expression of SCX (green spots, a) and SOX9 (red spots, b) proteins in healed rat ATEs. Merging the two images shows orange/yellow staining (c) indicating the presence of "fibrocartilage cells," which express both SCX and SOX9. These results are similar to those of intact rat ATEs (m, n, o, p). PRP treatment (e, f, g, h) increases the expression of SCX (green spots, e) but not SOX9, corroborating the theory that PRP alone mainly promotes tenogenesis resulting in collagen fibre formation but cannot induce fibrocartilage formation. Saline treatment does not induce SCX or SOX9 expression (i, j, k, l). The images of d, h, l, and p are enlarged views of the white boxes in c, g, k and o, respectively. (Immunohistochemical staining.)

excessive collagen III, which is typically disorganised, and weak in mechanical strength.

Interestingly, mechanical strength did not significantly differ between the KGN-PRP- and PRP-treated groups. In contrast, recently we found that the mechanical strength of the PRP-treated rat tendon graft-bone tunnels was less than that of the KGN-PRP-treated specimen.[38] A likely reason for this observation would be the experimental model used in this study. We created a 1 mm wound in the rat ATE and treated it with KGN-PRP or PRP alone. In such a model, the 1 mm wound is surrounded by a potentially larger area of uninjured tissue. Such disproportionate distribution of the injured area *versus* uninjured area may reduce the sensitivity of mechanical testing, and may in part explain the similar mechanical strength observed in the KGN-PRP- and PRP-treated ATEs. Therefore, tensile mechanical testing performed in this study alone cannot determine the quality of healing of the wounded ATE, because collagen I-rich fibres in the PRP treatment group exhibit tensile load-bearing capacity as good as the fibrocartilage region induced in the KGN-PRP group. The quality of healing must be judged not only by tensile mechanical testing, which measures the pull-out strength at the tendon-bone insertion site, but also by histological and immunohistological analyses of healed ATEs as done in this study.

The role of PRP in the healing of wounded rat ATEs in the KGN-PRP group may be related to the release of

KGN-PRP

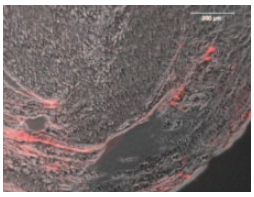

Fig. 9a

PRP

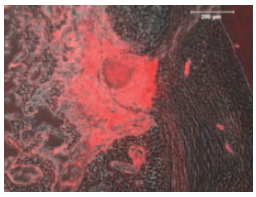

Fig. 9e

Saline

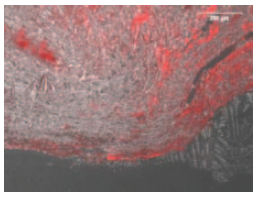

Fig. 9i

Intact

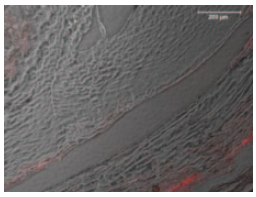

Fig. 9m

KGN-PRP

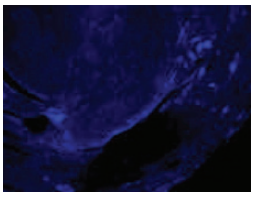

Fig. 9b

PRP

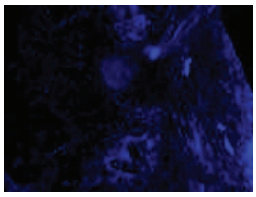

Fig. 9f

Saline

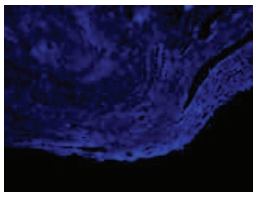

Fig. 9j

Intact

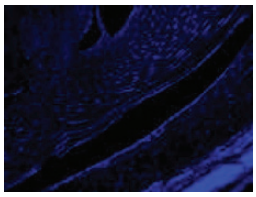

Fig. 9n

KGN-PRP

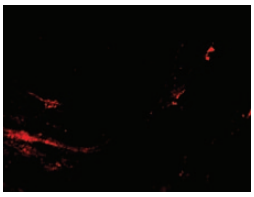

Fig. 9c

PRP

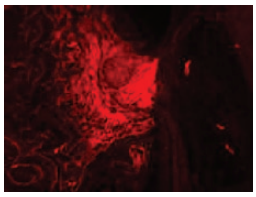

Fig. 9g

Saline

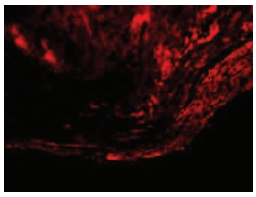

Fig. 9k

Intact

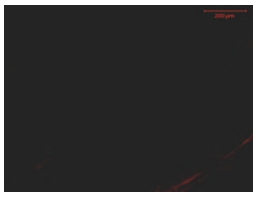

Fig. 9o

KGN-PRP

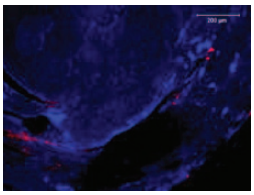

Fig. 9d

PRP

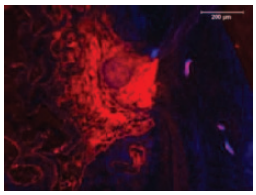

Fig. 9h

Saline

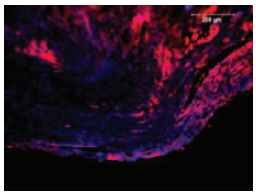

Fig. 9l

Intact

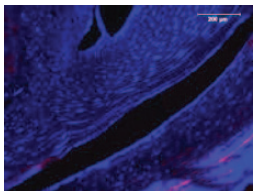

Fig. 9p

Collagen III expression in rat Achilles tendon entheses (ATEs) with various treatments. a to d) Kartogenin-platelet-rich plasma (KGN-PRP)-treated rat ATEs; e to h) PRP-treated rat ATEs; i to l) Saline-treated rat ATEs; m to p) intact (uninjured) rat ATEs. Collagen III expression is upregulated by saline- (red, i, j, k) or PRP- (red, e, g, h) treated rat ATEs. However, less than 5% of ATE tissues in both intact (red, m, o, p) and KGN-PRP-(red, a, c, d) treated ATEs are positively stained with collagen III (Immunohistochemical staining).

Table I. Scoring of healed rat Achilles tendon enthesis

Score	Kartogenin-platelet-rich plasma	Platelet-rich plasma	Saline	Intact
GAGs	3	1	0	4
SOX-9	3	1	1	4
Collagen II	3	1	1	4
Collagen III	0 to 1	3	3	0

growth factors contained in PRP gel, which are known to promote healing of injured tissues.[19,20] The effect of PRP in the KGN-PRP group may also be due to its ability to induce tenocyte differentiation of stem cells such as TSCs. Our previous study showed that PRP can promote proliferation and enhance tenocyte differentiation of TSCs.[32] While a large amount of data suggest that PRP is an excellent carrier and a healing promoter,[19,20,39,40] PRP alone is less effective in healing wounded entheses.[41] This may explain the finding of this study that PRP can promote healing of wounded ATEs, although its use alone cannot effectively promote fibrocartilage formation in the healing of wounded ATEs. To this end, KGN is required because it can induce chondrogenesis of stem cells and promote cartilage formation.[23]

Enthesis injuries often heal without regeneration of the fibrocartilaginous zone, thus increasing injury recurrence and also resulting in a high failure rate of tendon-bone

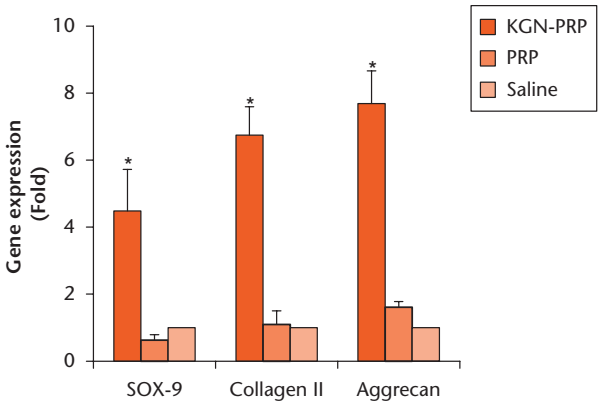

Fig.10a

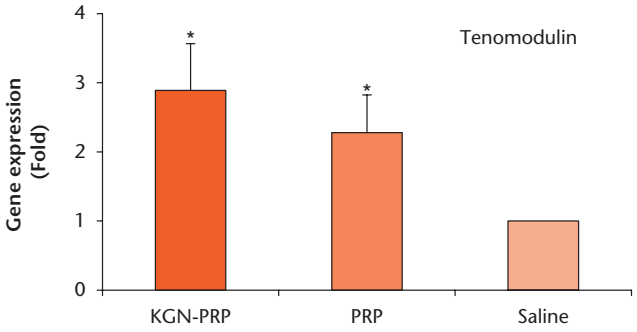

Fig.10b

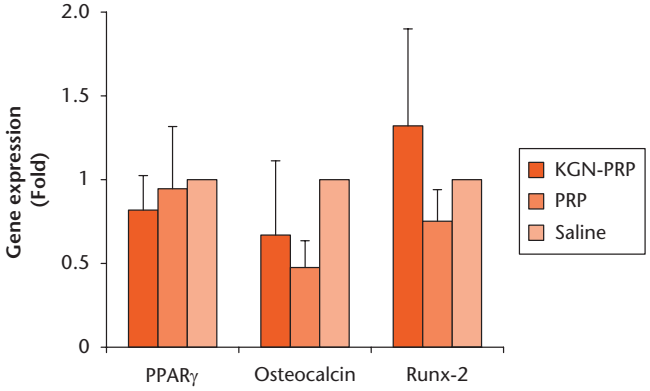

Fig.10c

Both chondrocyte- and tenocyte-related genes are expressed in the healed rat Achilles tendon entheses (ATEs) determined by quantitative real time polymerase chain reaction (qRT-PCR). Expression of a) chondrocyte-related genes, SOX9, collagen II and aggrecan, b) tenocyte-related gene, tenomodulin, and c) non-tenocyte-related genes, PPARγ, osteocalcin and RUNX2. Kartogenin-platelet-rich plasma (KGN-PRP) treatment significantly increases the gene expression of a) all three chondrocyte genes, and b) tenomodulin, but does not significantly affect the expression of c) non-tenocyte genes. PRP treatment does not significantly differ from saline treatment in the expression of a) chondrocyte genes or c) non-tenocyte genes. However, PRP significantly increases the expression of b) tenomodulin when compared with saline treatment. Data represent the mean SD of six samples from each group (*p < 0.05).

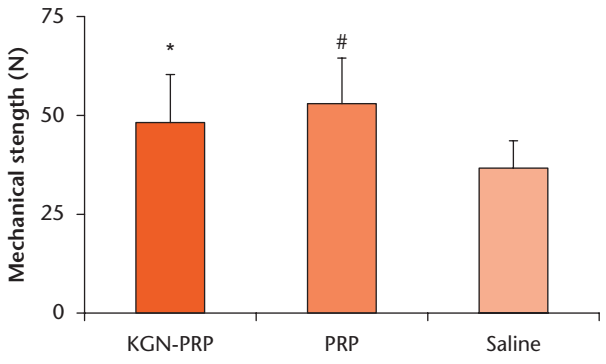

Fig. 11

Mechanical strength of the healed rat Achilles tendon entheses (ATE). Kartogenin-platelet-rich plasma (KGN-PRP) treatment increases the mechanical strength of the healed ATEs compared with the saline-treated ATEs. PRP treatment of wounded rat ATEs has a similar effect as KGN-PRP on the mechanical strength, which is estimated by measuring maximum failure load at the tendon insertion site. Data represents the mean and standard deviation of 14, 12, and eight specimens from KGN-PRP-, PRP-, and saline-treated groups, respectively (*p < 0.01 KGN-PRP *versus* saline; #p < 0.001 for PRP *versus* saline).

wound repair surgeries.[3,8,42] It has been reported that the failure rates of rotator cuff repairs, which require tendon-to-bone healing, are 20% for small tear repairs and 94% for massive tear repairs.[8,43] As shown in this study, the combined use of KGN and PRP may provide a novel tissue engineering approach to regenerate enthesis injuries.

The use of KGN-PRP to treat enthesis injuries has several advantages. First, KGN-PRP is a cell-free treatment modality that can be translated to clinical use with ease. Second, KGN serves as a biomolecule, which was previously shown to induce specific differentiation of stem cells such as MSCs mechanistically,[23] TSCs[24] and BMSCs[44] to chondrocytes when compared with other methods such as the use of MSCs or therapeutic ultrasounds. Third, KGN was previously shown to reduce degenerative changes in osteoarthritis rats.[44] Our studies on KGN further showed that KGN-PRP could enhance the tendon graft-bone tunnel healing in a rat model by increasing the fibrocartilage formation zone in the KGN-PRP-treated tendon-bone graft area.[38] Fourth, PRP in the KGN-PRP pair serves as a scaffold that functions as a "retainer" of KGN solution, thus preventing its diffusion into the surrounding tissues. The use of KGN alone without PRP will result in diffusion or 'leakage' that may lead to the formation of cartilage-like tissue in otherwise healthy tendon as shown in our previous study[45] and, as a result, may compromise tendon structure and function. Furthermore, PRP also has numerous growth factors that stimulate the healing of soft tissues[20,46] such as tendons,[47] and attracts other stem cells such as BMSCs that may further enhance tissue healing.[48] Others have also reported better treatment effects when a biocompound was conjugated with PRP.[49-51]

As mentioned above, in this study we used a partial injury model, meaning that the biopsy punch created only a 1 mm diameter wound in the inserted area. We chose this model because of the ease and accuracy in creating an ATE wound. However, this partial injury model differs from the total enthesis injury that often occurs in patients where the tendon is pulled out of the bone. Future studies should examine the efficacy of KGN-PRP on the complete transection model, which may be treated by first anchoring the tendon to bone followed by

KGN-PRP gel injection or implantation. An additional limitation of this study is the use of only one KGN concentration and one platelet concentration in KGN-PRP preparations. While both concentrations were based on our previous studies,[24,32] optimal doses of KGN-PRP in terms of KGN and platelet concentrations and the optimal delivery method (injection *versus* implantation) need additional investigations. Finally, although the mode of KGN action was shown to be through regulating the CBFβ–RUNX1 transcriptional programme,[23] the specific mode of action of KGN-PRP on the healing of wounded ATEs needs to be investigated. Another limitation of this study is that we used tensile mechanical testing to measure the mechanical strength of healed ATE. This is only an estimation, and precise *local* mechanical properties (e.g. compressive and shear strengths) of the wounded ATE after healing have to be determined by other means.

In conclusion, we have shown that injection of KGN-PRP enhanced healing of the wounded rat ATEs by promoting fibrocartilage formation. Thus, KGN can be used as a mode of cell-free therapy to promote regeneration of wounded entheses in clinical settings. PRP itself did not effectively promote fibrocartilage formation in our ATE model, but its use likely enhanced the healing of wounded rat ATEs.

References

1. **Apostolakos J, Durant TJS, Dwyer CR, et al.** The enthesis: a review of the tendon-to-bone insertion. *Muscles Ligaments Tendons J* 2014;4:333-342.
2. **Benjamin M, Toumi H, Ralphs JR, et al.** Where tendons and ligaments meet bone: attachment sites ('entheses') in relation to exercise and/or mechanical load. *J Anat* 2006;208:471-490.
3. **Juneja SC, Veillette C.** Defects in tendon, ligament, and enthesis in response to genetic alterations in key proteoglycans and glycoproteins: a review. *Arthritis* 2013;2013:154812.
4. **Evans RB.** Managing the injured tendon: current concepts. *J Hand Ther* 2012;25:173-189.
5. **Martinek V, Latterman C, Usas A, et al.** Enhancement of tendon-bone integration of anterior cruciate ligament grafts with bone morphogenetic protein-2 gene transfer: a histological and biomechanical study. *J Bone Joint Surg [Am]* 2002;84-A:1123-1131.
6. **Uhthoff HK, Seki M, Backman DS, et al.** Tensile strength of the supraspinatus after reimplantation into a bony trough: an experimental study in rabbits. *J Shoulder Elbow Surg* 2002;11:504-509.
7. **Woo SL, Hildebrand K, Watanabe N, et al.** Tissue engineering of ligament and tendon healing. *Clin Orthop Relat Res* 1999;367:S312-S323.
8. **Thomopoulos S, Genin GM, Galatz LM.** The development and morphogenesis of the tendon-to-bone insertion - what development can teach us about healing. *J Musculoskelet Neuronal Interact* 2010;10:35-45.
9. **He P, Ng KS, Toh SL, Goh JC.** In vitro ligament-bone interface regeneration using a trilineage coculture system on a hybrid silk scaffold. *Biomacromolecules* 2012;13:2692-2703.
10. **Nourissat G, Diop A, Maurel N, et al.** Mesenchymal stem cell therapy regenerates the native bone-tendon junction after surgical repair in a degenerative rat model. *PLoS One* 2010;5:e12248.
11. **Ramalingam M, Young MF, Thomas V, et al.** Nanofiber scaffold gradients for interfacial tissue engineering. *J Biomater Appl* 2013;27:695-705.
12. **Rothrauff BB, Tuan RS.** Cellular therapy in bone-tendon interface regeneration. *Organogenesis* 2014;10:13-28.
13. **Foster TE, Puskas BL, Mandelbaum BR, Gerhardt MB, Rodeo SA.** Platelet-rich plasma: from basic science to clinical applications. *Am J Sports Med* 2009;37:2259-2272.
14. **Marx RE.** Platelet-rich plasma: evidence to support its use. *J Oral Maxillofac Surg* 2004;62:489-496.
15. **Chen L, Dong SW, Tao X, et al.** Autologous platelet-rich clot releasate stimulates proliferation and inhibits differentiation of adult rat tendon stem cells towards nontenocyte lineages. *J Int Med Res* 2012;40:1399-1409.
16. **Kashiwagi K, Mochizuki Y, Yasunaga Y, et al.** Effects of transforming growth factor-beta 1 on the early stages of healing of the Achilles tendon in a rat model. *Scand J Plast Reconstr Surg Hand Surg* 2004;38:193-197.
17. **Parafioriti A, Armiraglio E, Del Bianco S, et al.** Single injection of platelet-rich plasma in a rat Achilles tendon tear model. *Muscles Ligaments Tendons J* 2011;1:41-47.
18. **Zhang J, Middleton KK, Fu FH, Im HJ, Wang JH.** HGF mediates the anti-inflammatory effects of PRP on injured tendons. *PLoS One* 2013;8:e67303.
19. **Alsousou J, Thompson M, Harrison P, Willett K, Franklin S.** Effect of platelet-rich plasma on healing tissues in acute ruptured Achilles tendon: a human immunohistochemistry study. *Lancet* 2015;385:S19.
20. **Anitua E, Sánchez M, Nurden AT, et al.** New insights into and novel applications for platelet-rich fibrin therapies. *Trends Biotechnol* 2006;24:227-234.
21. **Kütük N, Baş B, Soylu E, et al.** Effect of platelet-rich plasma on fibrocartilage, cartilage, and bone repair in temporomandibular joint. *J Oral Maxillofac Surg* 2014;72:277-284.
22. **Sun Y, Feng Y, Zhang CQ, Chen SB, Cheng XG.** The regenerative effect of platelet-rich plasma on healing in large osteochondral defects. *Int Orthop* 2010;34:589-597.
23. **Johnson K, Zhu S, Tremblay MS, et al.** A stem cell-based approach to cartilage repair. *Science* 2012;336:717-721.
24. **Zhang J, Wang JH.** Kartogenin induces cartilage-like tissue formation in tendon-bone junction. *Bone Res* 2014;2:2.
25. **Zhou Y, Wang J.** PRP Treatment Efficacy for Tendinopathy: A Review of Basic Science Studies. *Biomed Res Int* 2016:9103792.
26. **Del Bue M, Riccò S, Conti V, et al.** Platelet lysate promotes in vitro proliferation of equine mesenchymal stem cells and tenocytes. *Vet Res Commun* 2007;31:289-292.
27. **Chen L, Dong S-W, Liu J-P, et al.** Synergy of tendon stem cells and platelet-rich plasma in tendon healing. *J Orthop Res* 2012;30:991-997.
28. **Chen L, Liu JP, Tang KL, et al.** Tendon derived stem cells promote platelet-rich plasma healing in collagenase-induced rat achilles tendinopathy. *Cell Physiol Biochem* 2014;34:2153-2168.
29. **Eppley BL, Woodell JE, Higgins J.** Platelet quantification and growth factor analysis from platelet-rich plasma: implications for wound healing. *Plast Reconstr Surg* 2004;114:1502-1508.
30. **Filardo G, Kon E, Di Matteo B, et al.** Platelet-rich plasma injections for the treatment of refractory Achilles tendinopathy: results at 4 years. *Blood Transfus* 2014;12:533-540.
31. **Thanasas C, Papadimitriou G, Charalambidis C, Paraskevopoulos I, Papanikolaou A.** Platelet-rich plasma versus autologous whole blood for the treatment of chronic lateral elbow epicondylitis: a randomized controlled clinical trial. *Am J Sports Med* 2011;39:2130-2134.
32. **Zhang J, Wang JH.** Platelet-rich plasma releasate promotes differentiation of tendon stem cells into active tenocytes. *Am J Sports Med* 2010;38:2477-2486.
33. **Kang ML, Ko JY, Kim JE, Im GI.** Intra-articular delivery of kartogenin-conjugated chitosan nano/microparticles for cartilage regeneration. *Biomaterials* 2014;35:9984-9994.
34. **Pritzker KP, Gay S, Jimenez SA, et al.** Osteoarthritis cartilage histopathology: grading and staging. *Osteoarthritis Cartilage* 2006;14:13-29.
35. **Li M, Zhang J, Jin Q, et al.** Role of platelet-rich plasma in articular cartilage lesions. *Chin Med J (Engl)* 2014;127:3987-3992.
36. **Matson A, Konow N, Miller S, Konow PP, Roberts TJ.** Tendon material properties vary and are interdependent among turkey hindlimb muscles. *J Exp Biol* 2012;215:3552-3558.
37. **Thorsen S.** The mechanism of plasminogen activation and the variability of the fibrin effector during tissue-type plasminogen activator-mediated fibrinolysis. *Ann N Y Acad Sci* 1992;667:52-63.
38. **Zhou Y, Zhang J, Yang J, et al.** Kartogenin with PRP Promotes the Formation of Fibrocartilage Zone in the Tendon-Bone Interface. *J Tissue Eng Regen Med* 2017 [Epub ahead of print].
39. **Andia I, Latorre PM, Gomez MC, et al.** Platelet-rich plasma in the conservative treatment of painful tendinopathy: a systematic review and meta-analysis of controlled studies. *Br Med Bull* 2014;110:99-115.
40. **Cavallo C, Filardo G, Mariani E, et al.** Comparison of platelet-rich plasma formulations for cartilage healing: an in vitro study. *J Bone Joint Surg [Am]* 2014;96-A:423-429.
41. **Lamplot JD, Angeline M, Angeles J, et al.** Distinct effects of platelet-rich plasma and BMP13 on rotator cuff tendon injury healing in a rat model. *Am J Sports Med* 2014;42:2877-2887.
42. **Benjamin M, McGonagle D.** Entheses: tendon and ligament attachment sites. *Scand J Med Sci Sports* 2009;19:520-527.

43. **Aoki M, Oguma H, Fukushima S, et al.** Fibrous connection to bone after immediate repair of the canine infraspinatus: the most effective bony surface for tendon attachment. *J Shoulder Elbow Surg* 2001;10:123-128.
44. **Kang YH, Jeon SH, Park JY, et al.** Platelet-rich fibrin is a Bioscaffold and reservoir of growth factors for tissue regeneration. *Tissue Eng Part A* 2011;17:349-359.
45. **Zhang J, Wang JH.** PRP treatment effects on degenerative tendinopathy - an in vitro model study. *Muscles Ligaments Tendons J* 2014;4:10-17.
46. **DeLong JM, Russell RP, Mazzocca AD.** Platelet-rich plasma: the PAW classification system. *Arthroscopy* 2012;28:998-1009.
47. **Sánchez M, Anitua E, Azofra J, et al.** Comparison of Surgically Repaired Achilles Tendon Tears Using Platelet-Rich Fibrin Matrices. *Am J Sports Med* 2007;35:245-251.
48. **Rennert RC, Sorkin M, Garg RK, Gurtner GC.** Stem cell recruitment after injury: lessons for regenerative medicine. *Regen Med* 2012;7:833-850.
49. **Yamada Y, Ueda M, Hibi H, Nagasaka T.** Translational research for injectable tissue-engineered bone regeneration using mesenchymal stem cells and platelet-rich plasma: from basic research to clinical case study. *Cell Transplant* 2004;13:343-355.
50. **Wu W, Chen F, Liu Y, Ma Q, Mao T.** Autologous injectable tissue-engineered cartilage by using platelet-rich plasma: experimental study in a rabbit model. *J Oral Maxillofac Surg* 2007;65:1951-1957.
51. **Takikawa M, Nakamura S, Nakamura S, et al.** Enhanced effect of platelet-rich plasma containing a new carrier on hair growth. *Dermatol Surg* 2011;37:1721-1729.

Funding Statement
- This work was supported in part by the National Institutes of Health under award numbers AR061395, AR065949, and AR070340 (JHW).

Author Contribution
- J. Zhang: Designed research study, performed all *in vitro* and *in vivo* experiments, collected and analysed the data, drafted the paper.
- T. Yuan: Performed animal surgery, animal blood collection and PRP preparation
- N. Zheng: Performed mechanical testing and analysed results
- Y. Zhou: Performed animal surgery, KGN releasing experiment, and mechanical testing.
- M. V. Hogan: Analysed data and discussed their clinical relevance, edited the manuscript.
- J. H-C. Wang: Designed the research project, provided the reagents and equipment, analysed data, wrote and edited the manuscript.

ICMJE COI Statement
- None declared